

blood

Prepublished online April 19, 2011;
doi:10.1182/blood-2010-12-327346

Proteomic analysis identifies galectin-1 as a predictive biomarker for relapsed /refractory disease in classical Hodgkin lymphoma

Peter Kamper, Maja Ludvigsen, Knud Bendix, Stephen Hamilton-Dutoit, Gabriel A. Rabinovich, Michael Boe Møller, Jens R. Nyengaard, Bent Honoré and Francesco d'Amore

Information about reproducing this article in parts or in its entirety may be found online at:
http://bloodjournal.hematologylibrary.org/site/misc/rights.xhtml#repub_requests

Information about ordering reprints may be found online at:
<http://bloodjournal.hematologylibrary.org/site/misc/rights.xhtml#reprints>

Information about subscriptions and ASH membership may be found online at:
<http://bloodjournal.hematologylibrary.org/site/subscriptions/index.xhtml>

Advance online articles have been peer reviewed and accepted for publication but have not yet appeared in the paper journal (edited, typeset versions may be posted when available prior to final publication). Advance online articles are citable and establish publication priority; they are indexed by PubMed from initial publication. Citations to Advance online articles must include the digital object identifier (DOIs) and date of initial publication.

Blood (print ISSN 0006-4971, online ISSN 1528-0020), is published weekly by the American Society of Hematology, 2021 L St, NW, Suite 900, Washington DC 20036.

Copyright 2011 by The American Society of Hematology; all rights reserved.



Proteomic analysis identifies galectin-1 as a predictive biomarker for relapsed/refractory disease in classical Hodgkin lymphoma

Peter Kamper^{1,*}, Ph.D, Maja Ludvigsen^{2,*}, MS.c, Knud Bendix³, D.M.Sc., Stephen Hamilton-Dutoit³, FRCPath, Gabriel A. Rabinovich⁴, Ph.D., Michael Boe Møller⁵, D.M.Sc., Jens R. Nyengaard⁶, D.M.Sc., Bent Honoré^{2,**}, D.M.Sc., Francesco d'Amore^{1,**}, D.M.Sc.

1. Department of Hematology, Aarhus University Hospital, Aarhus, Denmark
2. Department of Medical Biochemistry, Aarhus University, Aarhus, Denmark
3. Institute of Pathology, Aarhus University Hospital, Aarhus, Denmark
4. Laboratorio de Inmunopatología, Instituto de Biología y Medicina Experimental (IBYME), Consejo Nacional de Investigaciones Científicas y Técnicas (CONICET), Buenos Aires, Argentina
5. Department of Pathology, Odense University Hospital, Odense, Denmark
6. Stereology & Electron Microscopy Laboratory, Center for Stochastic Geometry and Advanced Bioimaging, Aarhus University Hospital, Aarhus, Denmark

**** P.K. and M.L. contributed equally to this work.***

***** B.H. and F.d'A. contributed equally to this work.***

Running title: Galectin-1 as prognostic biomarker in cHL

Corresponding author

Peter Kamper, MD

Department of Hematology, Aarhus University Hospital, Tage Hansens Gade 2. DK-8000 Aarhus C

Phone: (+45) 89497560, Fax: (+45) 89497599

Email: petekamp@rm.dk

Abstract

Considerable effort has been spent identifying prognostic biomarkers in classical Hodgkin lymphoma (cHL). The aim of our study was to search for possible prognostic parameters in advanced stage cHL using a proteomics based strategy. A total of 14 cHL pretreatment tissue samples from younger, advanced stage patients were included. Patients were grouped according to treatment response. Proteins that were differentially expressed between the groups were analyzed using 2-dimensional polyacrylamide gel electrophoresis and identified by liquid chromatography mass spectrometry. Selected proteins were validated using Western blot analysis. One of the differentially expressed proteins, the carbohydrate-binding protein galectin-1 (Gal-1) was further analyzed using IHC and its expression was correlated with clinico-pathological and outcome parameters in 143 advanced stage cHL cases. At the univariate level, high Gal-1 expression in the tumor microenvironment correlated with poor event-free survival ($p=0.02$). Among younger (≤ 61 yrs) patients, a high Gal-1 correlated with poorer overall and event-free survival (both $p= 0.007$). In this patient group and at the multivariate level, high Gal-1 expression retained a significant predictive impact on event-free survival. Thus, in addition to its functional role in cHL-induced immunosuppression, Gal-1 is also associated with an adverse clinical outcome in this disease.

Introduction

The tumor lesion in classical Hodgkin lymphoma (cHL) is characterized by the presence of the typical Hodgkin and Reed-Sternberg (HRS) tumor cells, largely outnumbered by non-neoplastic inflammatory bystanders that include B- and T-lymphocytes (predominantly Th2-type and FoxP3+ regulatory T cells), macrophages, eosinophils, basophils and plasma cells¹.

Over the last decades, the treatment of cHL has improved considerably and current therapeutic strategies succeed in curing more than 80% of patients. However, 20-30% still experience relapse or refractory disease, many subsequently succumbing to death as a result of either treatment complications or disease progression². Prompted by observations in other lymphoma subtypes, e.g. follicular lymphoma³, increased attention has been drawn to the possible biological role and prognostic significance of the tumor-infiltrating inflammatory cells in cHL. A number of recent studies have focused on this area, using gene expression profiling to identify new prognostic markers in cHL^{4;5}. Although these studies have led to the identification of a number of candidate genes, no specific biological marker has yet been introduced as a reliable tool for pre-therapeutic risk assessment.

A number of factors may influence the proteomic machinery and affect the final properties of the encoded protein at several levels: translational inhibition/activation, posttranslational modifications, inhibition/activation of the proteins, specific degradations, etc. Consequently, there can be considerable discrepancy between the expression level of RNA and that of the corresponding protein product⁶. Therefore, proteomics-based approaches have recently been used in HL in order to identify protein patterns that may provide pathogenetic and prognostic

clues^{7;8}. However, these studies were only performed in cell lines and still await confirmation in an *in vivo* setting.

Galectin-1, a member of a growing family of animal lectins with affinity to poly-*N*-acetyllactosamine-enriched glycoconjugates, has recently emerged as a regulator of inflammatory responses, angiogenesis and tumor progression^{9;10}. This glycan-binding protein has been identified as a critical mediator of the immunosuppressive activity of cHL, being responsible for creating the Th2-Treg skewed microenvironment typical of the disease^{11;12}. Moreover, the combination of galectin-1 and c-Jun has been proposed as a diagnostic biomarker for distinguishing cHL from other lymphomas with shared morphologic and molecular features¹³.

The aim of the present study was to provide data from an “*in vivo*” setting by identifying differentially expressed proteins in primary diagnostic tissue samples from treatment-sensitive vs. treatment-refractory cHL patients. This study constitutes the first approach seeking to correlate protein expression as assessed by proteomics, with treatment response and clinical outcome in advanced stage cHL. Protein expression was evaluated in both the neoplastic and non-neoplastic compartments of tumor biopsies.

Patient and Methods

Patients

A total of 14 cHL pretreatment tissue samples were selected for 2-dimensional polyacrylamide gel electrophoresis (2D-PAGE) and liquid chromatography – tandem mass spectrometry (LC-MS/MS). The tissue samples were embedded in Tissuetek® OCT™ compound and snap-frozen in isopentane in liquid nitrogen at the time of diagnosis, and were subsequently stored at -80°C.

On the basis of responses to initial treatment, two patient cohorts were identified. The clinical features of these patients are detailed in Table I. One cohort was characterized by a favorable treatment response, i.e. sustained complete remission (CR) for a minimum of 36 months. The second was characterized by an unfavorable response to treatment, i.e. either progressive/refractory disease or relapse within a year after end of first-line therapy. In order to maximize comparability between the two cohorts in terms of protein expression, patients in the two groups were matched with regard to age (range 20-35 vs. 14-51, median 24 vs. 27 years; $p=0.52$), clinical stage (IB, IIB, III or IV), and cHL histology, i.e. nodular sclerosis (NS) or mixed cellularity (MC). The workflow is outlined in Fig.1.

Where possible, data generated from the proteomic analysis were validated in a cohort of 143 cHL patients using immunohistochemistry (IHC) on tissue microarrays (TMAs) constructed from formalin-fixed paraffin-embedded primary pre-treatment tumor biopsies (Table 2). Clinical and follow-up data were obtained from clinical records. For deceased patients, the precise date of death was obtained from the Danish Civil Registration System. All primary diagnostic tumor biopsies were reviewed and reclassified according to the WHO classification of tumors of the haematopoietic and lymphoid tissues¹⁴. The patients were treated at Aarhus University Hospital between 1990 and 2007 according to standard guidelines. Patients were uniformly treated with ABVD/COPP (adriamycin, bleomycin, vinblastine, dacarbazine/cyclophosphamide, vincristin, procarbazine, prednisone) chemotherapy. Additional radiotherapy was given in case of pre-therapeutic bulk or localized residual masses. Treatment response was assessed using standardized guidelines¹⁵. The study was approved by the Regional Ethical Committee and by the Danish Data Protection Agency.

Sample collection and preparation

From each cHL sample, a total of 70 sections of 20 μm were cut and transferred into empty Eppendorf tubes. Hematoxylin and eosin (H&E) stains were made before and after this process to ensure the presence of HRS cells throughout the samples. Subsequently, 350 μl 3-10 NL lysis buffer (9M urea, 2% (wt/vol) Triton X-100, 2% (wt/vol) dithiothreitol, 2% (vol/wt) IPG-buffer (Amersham)) were added to the cut sections.

Determination of total protein content

In order to ensure loading of equal protein amounts for both 2-D PAGE and 1-D western blotting, the protein concentration was determined using a non-interfering assay (488250, Calbiochem, EMD, Gribbstown, NJ).

Two-dimensional polyacrylamide gel electrophoresis (2D-PAGE)

The 2D-PAGE procedure was performed essentially as described^{16;17} with a few modifications. In summary, 100 μg protein was used from each sample. Isoelectric focusing (IEF) was performed using 18 cm pH 3–10 or pH 4-7 non-linear IPG-strips. The IPG strips were rehydrated overnight (approximately 20 hours) in 150 μl rehydration solution (8 M urea, 2% (wt/vol) CHAPS, 0.3% (wt/vol) DTT, 2% (vol/wt) IPG-buffer, bromphenol blue) together with the 100 μg protein sample in 200 μl 3-10 NL lysis buffer in a Immobiline DryStrip Reswelling Tray. After rehydration, the samples were run at 500 V 1 min, 500 V 5 h and 3500 V 14.5 h (Multiphor II system, Perkin Elmer Windsor, UK) in a gradient mode at 17°C (MultiTemp III Thermostatic Circulator; GE Healthcare Life Sciences, Buckinghamshire, UK). The IPG strips were equilibrated twice: first in 20 ml equilibration buffer (0.6% (wt/vol) Tris-HCl (pH 6.8), 6 M urea, 30% (vol/vol) glycerol, 1% (wt/vol) SDS, and 0.05% (wt/vol) DTT) and secondly in 4.5% (wt/vol) iodoacetamide and

bromophenol blue. For the second dimension, 12% polyacrylamide gels were used (sodiumdodecylsulphate PAGE). The gels ran at 50 V overnight (approximately 20 hours). They were transferred to fixation solution (50% ethanol, 12% acetic acid, 0.05% formaldehyde) for a minimum of 1 h.

Silver Staining

In order to visualize the proteins separated by 2-D PAGE, we used the Vorum protocol as previously described¹⁸. Gels were washed three x 20 min in 35% ethanol, then pretreated for 2 min in 0.02% Na₂S₂O₃·5H₂O and washed in H₂O x three for 3 min each. The gels were stained with 0.2% AgNO₃, 0.028% formaldehyde for 20 min. Gels were then rinsed twice in H₂O for 1 min. Gels were then developed in 6% Na₂CO₃, 0.0185% formaldehyde, 0.0004% Na₂S₂O₃·5H₂O and the reaction was stopped using 40% (vol/vol) ethanol and 12% (vol/vol) acetic acid. This solution was changed once and the gels were dried between cellophane sheets and sealed.

Data analysis

Two analyses were performed with first dimension separation using isoelectric focusing at either pH 3-10 or pH 4-7. Thirteen patients were included in each analysis. (pH 3-10: Patient 27; 35; 69; 79; 138; 174; 182; 201; 243; 333; 415; 463; 464, pH 4-7: Patient 35; 69; 79; 138; 174; 182; 201; 243; 333; 415; 462; 463; 464). The gels were scanned with a GS-710 Calibrated Imaging Densitometer (BioRad, Hemel Hempstead, UK) using the Quantity One software package. Gels were then imported into the PDQuest Advanced 2-D Gel Analysis Software (BioRad, Hemel Hempstead, UK) that assigned a volume to each spot proportional to the amount of protein. In short, the gels were normalized against the total density and, after background subtraction, the spots were automatically defined and quantified. One gel in each study (pH 3-10: patient 79; pH

4-7: Patient 464) was chosen as a reference gel (master gel). In the reference gel, each spot was assigned a number and all other gels were aligned to the reference gel and all matched spots were numbered accordingly. All matches were critically evaluated and necessary editions and corrections were performed manually. Spots that showed a significant (Mann-Whitney *U* test, $p < 0.05\%$) and at least two-fold differential expression were cut out of the gel and subjected to in-gel tryptic digestion.

Protein identification by LC-MS/MS

Sample preparation and mass spectrometry were performed essentially as described¹⁹. In summary, proteins were in-gel trypsinized overnight, pre-treated with acetonitrile, reduced with DTT and blocked with iodacetamide, cleaved by trypsin and the peptides were extracted by one change of NH_4HCO_3 and 3 changes of formic acid in acetonitrile. Finally, the extracted peptides were dried. The dried fragmented protein samples were dissolved in 6 μl buffer A (97.7% H_2O , 2% acetonitrile, 0.3% formic acid). Peptide separation before MS/MS analysis was performed using an inert nano liquid chromatography system (LC Packings (San Francisco, CA)). The samples were then analysed on a Q-TOF Ultima mass spectrometer (Micromass, Manchester, UK). The processed data were used to search the Swiss-Prot Database (version 57.7, 57.8 or 2010_12 containing 497.293, 509.019 or 523.151 sequences) or in a few cases the mammalian part (64,853 sequences) or human the part (20,405 sequences) using the on-line version of the Mascot MS/MS Ion Search facility (Matrix Science, Ltd., <http://www.matrixscience.com>)²⁰. Searching was performed with doubly and triply charged ions with two missed cleavages, a peptide mass tolerance of 20 or 50 ppm and an MS/MS tolerance of 0.05 Da.

Antibodies

The primary rabbit polyclonal anti-galectin-1 antibody generated in the laboratory of one of the authors (GAR), has previously been described and found to be specific for Gal-1 detection in cHL¹³ (Western Blotting (WB) dilution 1:100; IHC dilution 1:5000). Other antibodies used were purchased from commercial suppliers: anti-PSME1 (HPA006632; WB dilution 1:100, IHC dilution 1:400; ATLAS antibodies, Stockholm, Sweden), anti-GNAI3 (XW-7212; WB dilution 1:200 ProSci Incorporated, Poway, CA) and anti-Prdx1 (HPA007730; WB dilution 1:100, IHC dilution 1:75; Atlas Antibodies, Stockholm, Sweden), anti-FOXP3 (clone 236A/E7, dilution 1:50, Biocare Medical, CA, USA), anti-granzyme-B (clone GrB-7, dilution 1:20, DAKO, Glostrup, Denmark), anti-CD68 (clone KP-1, dilution 1:800; Dako, Glostrup, Denmark), anti-CD163 (clone 10D6, dilution 1:50; Novocastra, Newcastle, UK), and anti-latent membrane protein-1 (LMP-1) (clones CS 1-4, dilution 1:100; DAKO, Glostrup, Denmark).

Western blotting (WB)

WB was carried out in 12 out of 14 patients from the cohort. One patient per cohort could not be analyzed due to the limited amount of protein left after the 2D-PAGE experiments. The same amount of protein was added to each lane of the western blots used for one comparison, either 5 microgram per lane in case of galectin-1 or 10 microgram per lane in case of guanine nucleotide-binding protein G(k) subunit alpha (GNAI3), peroxiredoxin-1 (PRDX1), proteasome activator complex subunit 1 (PSME2) and desmoplakin (DESP). The samples were loaded on Novex© 10–20% Tris-glycine Gel, 1.0 mm, 10 well, (Invitrogen, Carlsbad, CA) and run for 2 h at 125 V. After transfer by electroblotting (200 mA for 2 h) to Hybond-H Extra, nitrocellulose, 0.45 mm. (Amersham Biosciences/GE Health care, Pittsburgh, PA), the blots were blocked with 5% skim

milk in PBS-T (0.05% Tween-20 in 80 mM Na₂HPO₄, 20 mM NaH₂PO₄, 100 mM NaCl, pH 7.5) and incubated overnight at 4°C. The blots were washed 3 times in PBS-T and incubated 1 h with the primary antibody, then washed again 3 times in PBS-T and incubated with horseradish peroxidase-conjugated secondary antibodies (P217, P260 DAKO, Glostrup Denmark or ab16349, Abcam Cambridge, UK; diluted 1:5000). Development of blots was done by using the enhanced chemiluminescence system, Amersham International, preceded by 4 PBS-T washes. Digital photos were taken and analyzed by Fujifilm LAS-3000 and Image Reader LAS-3000, (Fuji, Tokyo, Japan). Quantification of the bands in the western blots was done with the Multi Gauge V3.0 analysis program (FUJIFILM, Tokyo, Japan). In short, boxes are created around each band and a background box is made in a reference area. The pixel intensities are measured and the mean of the pixel intensity from the reference area is subtracted from each pixel in the bands. Then the intensities of the bands are analyzed with a Mann-Whitney U-test to find significant differences (p<0.05).

"Housekeeping" proteins are often used as reference proteins to check for proper analyses of the western blots since the expression of these proteins are assumed to be at constant level under varying conditions. However, there is increasing evidence in proteomic studies that "housekeeping" proteins such as, e.g., actin, tubulin and GAPDH may be inadequate as internal standards since the expression can be affected by a large number of factors^{19;21-23}. Our present observations are in line with these findings, since we found two often used "housekeeping" proteins, actin and GAPDH, to be differentially expressed in tumor biopsies. Therefore, they were not considered adequate as reference proteins in the present study. Instead, we chose to normalize the western blots to the total protein concentration present in the tumor sample. For this purpose, the protein concentration was measured by using a non-interfering protein assay (see "Determination of total protein content").

Immunohistochemistry and *in situ* hybridization (ISH)

IHC staining was performed using 4 µm paraffin-embedded tissue sections. Gal-1, FoxP3, granzyme-B, CD68, CD163 and LMP-1 stainings were performed on the Ventana Benchmark automated staining system (Ventana Medical Systems, Tucson, AZ). For PRDX1 the Xmatrix automated staining system (Biogenex Laboratories, San Ramon, CA) was used. The staining for PSME1 was performed manually. Slides were incubated with the primary antibodies for 32 min (Gal-1, PSME1, FoxP3, granzyme-B, CD68, CD163, LMP-1) or 60 min (PRDX1) at 37°C. For primary antibody detection the Ventana Ultraview™ DAB detection kit and the DAKO Envision™ Flex⁺ visualization system were used. Tissues from malignant melanoma (Gal-1), tonsil tissue (FoxP3, Granzyme-B), colon (PSME1), lung (PRDX1), liver (CD68, CD163) and EBV+ cHL specimens (LMP-1, EBER) were used as positive controls. The primary antibodies were omitted in negative controls. For LMP-1 staining, the signal was enhanced with a Ventana amplification kit. Slides were counterstained with hematoxylin. Non-isotopic ISH for Epstein-Barr virus (EBV)-encoded RNAs 1 and 2 (EBER) was performed and scored as described²⁴.

Tissue microarray construction

TMA blocks containing triplicate 1 mm cores from each patient paraffin embedded sample were constructed with a manual tissue microarrayer (Beecher Instruments, Sun Prairie, WI), according to standard guidelines²⁵. Each block also contained samples of normal lymph node, placenta, kidney, and liver tissue as internal controls and guides.

Quantification of Gal-1 expression in HRS cells

Case in which more than 50 % of the HRS cells reacted with the antibody were considered positive. Intra-observer variation was estimated in 30 patients and the match between readings was found to be excellent with an overall agreement of 89%.

Quantification of Gal-1 expression in non-neoplastic bystander cells

Quantification of immunohistochemical stained sections was performed by stereological analysis using a light microscope equipped with a computer assisted stereology system (CAST, Visiopharm, Hoersholm, Denmark). The microscope had a motorized stage controlled by a computer for systematic uniform random sampling of fields of view. A Gal-1 positive cell profile in the tumor microenvironment was defined as nuclear staining of any non-HRS cell in the tumor microenvironment, e.g. macrophages, plasma cells, lymphocytes or endothelial cells. A minimum of approximately 100 Gal-1 positive cell profiles was counted from each patient sample (median for the entire cohort: 232). Cell profiles were counted with a 40 x lens at a final screen magnification of 1423, using a 2D unbiased counting frame²⁶. Areas containing either necrosis or artefacts were ignored. In order to evaluate the intra-observer variation, the Pearson correlation coefficients were calculated in a subset of patients (n=30). The correlation coefficient was found to be 0.91 and, in accordance with a cut-point between the third and fourth quartile, the percentage of correctly classified samples was 93%. The numbers of FoxP3 and granzyme-B positive cell profiles per mm² were quantified in a similar manner. The CD68⁺ or CD163⁺ volume fraction was determined by point-counting with a 20 x lens at a total magnification of 739x.

Statistical analysis

Patient characteristics were compared using the Wilcoxon rank-sum test, Kruskal-Wallis equality-of-populations rank test and χ^2 when appropriate. The follow-up time was defined as the time from diagnosis to either last follow-up or a given event. Event-free survival (EFS) was measured from the date of diagnosis to either disease progression or relapse, or discontinuation of treatment for any reason or censoring date. Overall survival (OS) was measured from the date of diagnosis to the date of death for any reason or censoring date. For correlation of patient survival and Gal-1 expression, patients were grouped into quartiles. The quartile of patients with the highest Gal-1 expression was also analyzed against the lower three quartiles taken as one group. This corresponded to a cut point of 1825 cell profiles/mm², which was used throughout the data analysis. Survival was estimated by the Kaplan-Meier method and compared using a log-rank test. A Cox proportional multivariate model was used to assess the possible association between Gal-1 and OS and EFS, while adjusting for those factors, which had a significance level <0.10 at the univariate level. Prior to the Cox regression analysis, the assumption of proportional hazards was assessed graphically. Correlation between continuous variables was done using Kendall's correlation. Two-sided *p*-values < 0.05 were considered statistically significant and *p*-values <0.10 were considered as borderline significant. All statistical analyses were done using STATA software version 10.1 (STATA, TX, USA).

Results

Identification of differentially expressed proteins using 2D gel-electrophoresis (2-DE) and LC-MS/MS

Fig. 2 shows representative 2D gels from the pH 3-10 IPG and pH 4-7 IPG experiments. In total, 37 protein spots were found to be differentially expressed in patients with advanced stage Hodgkin lymphoma. All of these were excised and analyzed for protein identification. Using LC-MS/MS and a subsequent search in the Swiss-Prot Database, 18 spots resulted in clear protein identification. Six of these spots contained more than one protein; e.g. spot 4302 contained both the Ig lambda chain C region and actin. Moreover, some proteins were identified in more than one spot, e.g. peroxiredoxin-1 in two spots (8206 and 8208). Table 2 summarizes the identification information including protein name, accession number, molecular weight, Mascot score and function. Four of the listed proteins were further validated by Western blot analysis.

Validation of proteomic analysis by Western blot

Fig. 3 shows Western blot analysis of five proteins differentially expressed in the two patient cohorts: galectin-1 (Gal-1), guanine nucleotide-binding protein G(k) subunit α (GNAI3), peroxiredoxin-1 (PRDX1), proteasome activator complex subunit 1 (PSME1) and desmoplakin. Integrative analysis confirmed the differential expression of these five proteins in patient samples. However, Gal-1 was the only protein that was significantly upregulated in treatment refractory patients ($p=0.01$). The remaining three proteins showed either a significant (GNAI3, $p=0.0003$; PRDX1, $p=0.02$) or a trend-like non-significant (PSME1, $p=0.11$; desmoplakin, $p=0.052$) upregulation in patients with favorable outcome.

Immunohistochemical localization of Gal-1, PSME-1 and PRDX1 in cHL microenvironment

Fig. 4 illustrates representative immunohistochemical stainings for Gal-1, PSME-1 and PRDX1. Cytoplasmatic and nuclear Gal-1 labeling were found in HRS cells, lymphoma-associated macrophages (LAMs) and endothelial cells in line with previous reports^{12;13} (Fig. 4a). Furthermore, we also noted a positive nuclear/cytoplasmatic reaction in some plasma cells. Most tumor-infiltrating lymphoid cells were Gal-1 negative. PSME1 immunostaining demonstrated a combined cytoplasmatic/nuclear positivity in both tumor and non-neoplastic by-stander cells (Fig. 4b). PRDX1 was also found to be weakly expressed by HRS cells. The signal localization was primarily cytoplasmatic. With regard to the tumor microenvironment, PRDX1 was predominantly expressed in LAMs (Fig. 4c).

Clinico-pathological features of TMA cohort patients

The main clinical and histopathological features of the study cohort are summarized in Table 3. The patient population had a median age of 35 years and a male/female ratio of 1.8. The median follow-up was 7 years (range: 0.2-18.6 years). The majority of the patients (60%) had stage III-IV disease, while 40% presented with a lower clinical stage (I-II), but with concomitant B-symptoms as a probable sign of more advanced disease. The large majority of the patients in the study cohort (82%) had B-symptoms at presentation and the median IPS score was 2. Approximately one third of the patients had EBV-positive tumors. The large majority (84%) displayed histological features consistent with the NS subtype.

Correlation of Gal-1 expression in neoplastic and non-neoplastic cells with demographic and clinico-pathological features

A total of 78 patients (55%) showed Gal-1 positivity in HRS cells. Interestingly, we found that cases with a high expression of Gal-1 in HRS cells frequently presented with B-symptoms at diagnosis ($p=0.002$). Gal-1 expression in HRS cells correlated with histologic subtype. Furthermore, with respect to the expression of Gal-1 in non-neoplastic cells only one significant correlation was found, high expression of Gal-1 being correlated with the presence of B symptoms ($p=0.03$) (Table 3).

Correlation of Gal-1 expression in neoplastic and non-neoplastic cells with patient survival in Hodgkin lymphoma

Patient survival (OS as well as EFS) was correlated to age with higher survival in the group of patients <45 years. Several other clinico-pathological parameters showed no correlation with survival. With respect to Gal-1 expression, there was no correlation between Gal-1 expression in HRS cells and OS or EFS (results not shown). Interestingly, a high Gal-1 expression in the tumor microenvironment significantly correlated with poor EFS ($p=0.02$) (Table 4). Among the younger, transplant-eligible patient population (< 61 years), the adverse impact of a high number of Gal-1-positive cell profiles on outcome was more pronounced. EFS and OS for low vs high Gal-1 expression were 90 % vs 78% ($p=0.007$) for the former and 69 % vs 49% ($p=0.007$) for the latter endpoint. Survival curves are shown in Fig. 5. In this younger patient population, high Gal-1 values retained their significant impact on EFS ($p=0.005$) at multivariate level. The predictive value of Gal-1 expression in younger patients (≤ 61 yrs) persisted also in terms of both EFS and OS despite of the concomitant presence, in the Cox regression model, of macrophage-related

parameters such as high CD68 (p values: 0.009 and 0.02, respectively) or high CD163 expression (p values: 0.02 and 0.003, respectively).

Correlation between Gal-1 expression in the non-neoplastic cells and tumor-infiltrating inflammatory cells of Hodgkin lymphoma patients

We further examined the correlation between Gal-1 expression and the tumor inflammatory infiltrate characteristic of cHL. With regard to the tumor microenvironment Gal-1 positivity correlated with the level of macrophage marker expression, in particular the M2 macrophage marker CD163 ($p=0.0007$) and, to a lesser extent, the pan-macrophage marker CD68 ($p=0.052$). This result is relevant in terms of the ability of Gal1 to foster the differentiation of alternatively-activated macrophages and tolerogenic dendritic cells²⁷⁻²⁹. Furthermore, a significant correlation between Gal-1 and granzyme B⁺ cytotoxic T lymphocytes was found ($p=0.02$). Conversely, no correlation with FoxP3⁺ T regulatory cells was detected ($p=0.26$) in spite of the abundant expression of Gal1 in FoxP3⁺ T regulatory cells³⁰.

Discussion

The Human Genome Project has revealed that the number of proteins in the human proteome exceeds by far the number of protein-coding genes in the human genome (~400,000 proteins versus ~30,000 genes)³¹. Because proteins are the functional end-product, it seems more appropriate to search for potential tumor biomarkers at the protein rather than gene level. Previous studies in lymph nodes and lymphoma samples have shown that the 2-D gel-based proteomics approach was feasible and reproducible³². Furthermore, it was demonstrated that this technique yielded similar results, irrespective of whether fresh biopsies or frozen samples that had been stored up to one year were used. Subsequently, this methodology was applied in order

to compare mantle cell lymphoma samples and inflammatory lymph node tissue, resulting in the identification of a number of differentially-expressed proteins³³. In our study, we were able to demonstrate the feasibility of using archival whole-tumor, frozen tissue from cHL patients for proteomic analysis. In spite of the fact that some of these samples had been stored for more than 10 years they still yielded technically satisfactory results. Proteomic-based expression profiles of the two patient groups selected on the basis of their response to treatment successfully identified proteins of prognostic value that are differentially expressed between these two groups.

The glycan-binding protein Gal-1 has been previously implicated as a modulator of the biology cHL. Expression of this protein by Reed Sternberg cells has been demonstrated to confer immune privilege to cHL cells, creating an appropriate niche for tumor progression. On the basis of gene expression profiling, Gal-1 was found to be over-expressed in HRS cell lines and its secretion favored a Th2 type immune response characterized by high IL-4 and IL-13 secretion and promoted expansion of CD4⁺CD25⁺FoxP3⁺ regulatory T cells¹². Moreover, exposure to recombinant Gal-1 inhibited proliferation and IFN- γ secretion by EBV-specific T cells¹¹, and T cells specific for EBV-LMP1 were much more susceptible to Gal-1-mediated immunosuppression than conventional T cells³⁴ suggesting a critical role for Gal-1 in compromising cHL-specific immunity. Supporting these findings, Gal-1-deficient (*Lgals1*^{-/-}) mice were found to be highly susceptible to Th1 and Th17-dependent inflammation as compared to their wild-type counterparts³⁵. Subsequent studies have shown that Gal-1 expression is not only seen in HRS cells, but is also abundant in the tumor microenvironment¹³. The latter observation was confirmed by our study, although correlation between Gal-1 expression and FoxP3 upregulation could not be demonstrated at the level of primary biopsies.

An important finding of the present study was the identification by proteomic analysis of Gal-1 among the proteins that are differentially expressed in treatment-refractory disease. This observation was further substantiated by immunohistochemical analysis which unambiguously showed a correlation between Gal-1 expression within the tumor microenvironment and poor clinical outcome. This impact was much more evident among younger patients (≤ 61 years), and persisted for EFS following a multivariate analysis. Considering the fact that Gal-1 is expressed in macrophages and that macrophages have recently been shown, also by our group, to predict a poor prognosis^{5,36,37}, it seemed relevant to test whether the adverse prognostic impact of Gal-1 also would persist in the presence, within the Cox regression model, of parameters associated with the number of macrophages, i.e. CD68 or CD163 positivity. The predictive value of Gal-1 expression in younger patients (≤ 61 yrs) was retained in terms of both EFS and OS despite of the concomitant presence of high CD68 or high CD163 expression, suggesting that the prognostic impact of high Gal-1 expression is not a mere reflection of the number of macrophages in the tumor tissue.

In addition to Gal-1, we identified in the pilot study PRDX1 and GNAI3 among proteins that were substantially up-regulated in patients with a favorable outcome. PRDX1 is a member of the peroxiredoxin family of antioxidant enzymes, which reduces hydrogen peroxide and alkyl hydroperoxides. In addition to its role as an anti-oxidant, it has been shown to enhance the cytotoxicity of natural killer (NK) cells³⁸. Interestingly, PRDX1-null mice develop hemolytic anemia (due to accumulation of reactive oxygen species) and a variety of malignancies including lymphomas. For this reason, it has been suggested that this protein plays an antioxidant protective role and may function as a tumor suppressor³⁹.

GNAI3 belongs to the guanine nucleotide-binding proteins (G-proteins) that are important regulators of Akt mediated cell migration⁴⁰, a critical process that contributes to shape the tumor microenvironment. Many cytokines and chemoattractants signal through the Akt/PKB pathway at the leading edge of migrating cells⁴¹.

All differentially expressed proteins identified on the basis of the proteomic analysis are currently being investigated in a validation setting. Therefore, as long as the result of the validation studies is still pending, it is premature to formulate prognostic statements with regard to these additional differentially expressed proteins.

In summary, our study confirms the feasibility of using archival frozen tissues from cHL patients for proteomic analysis. The two clinical groups analyzed showed relevant differences in their protein expression profile. Whilst the immunoregulatory glycan-binding protein Gal-1 was up-regulated in patient subsets with poorer outcome, PRDX1, a member of a family of antioxidant enzymes and GNAI3, a cell migration-associated protein, were identified among proteins that were substantially up-regulated in patients with a favorable outcome. In cHL (as in certain non-Hodgkin lymphoma subtypes) there is now substantial evidence to show that the tumour microenvironment plays an important role in the biology and prognosis of the disease^{42;43}. Our study contributes further evidence to support this hypothesis identifying Gal-1 as a potential novel biomarker that may be useful in the prognostic and predictive analysis of cHL. The study also underlines the advantages of proteomics in providing important clues to identify new therapeutic, diagnostic and prognostic targets in hematological malignancies.

Acknowledgements

The authors wish to thank Mette Hjøllund Christiansen, Kristina Lystlund Lauridsen Mona Britt Hansen, Inge Kjærgaard Nielsen and Tom Nordfeld for technical assistance, collaborating pathological departments for retrieval of tissue samples and Jens Overgaard and the Department of Experimental Oncology for scientific inspiration and logistic support. The authors are also grateful to Professor Margaret Shipp, Dana Farber Cancer Institute, Boston, Massachusetts for scientific advice.

Financial support

This work was supported by Aarhus University, the Karen Elise Jensen Foundation, the Max and Inger Wørzner Foundation, the Foundation in Commemoration of Eva and Henry Frænkel, the Aase and Ejner Danielsen Foundation, the Poul and Ellen Hertz Foundation; the Else and Mogens Wedell-Wedellsborg Foundation, the A.P. Møller and Chastine Mc-Kinney Møller Foundation for General Purposes, the Danish Cancer Research Foundation, the John & Birthe Meyer Foundation, Aarhus University Research Foundation and the Medical Research Council. The Centre for Stochastic Geometry and Advanced Bioimaging is supported by Villum Foundation.

Author contributions

PK, ML, KB, SHD, GAR, BH, JRN and FDA contributed to the design of the study; KB, SHD and MBM provided the study material; PK, KB, SHD and MBM reviewed all cases; GAR contributed with vital reagents. PK, ML, BH performed the laboratory work; PK, ML, BH, JRN and FDA participated in the data analysis and interpretation. PK, ML, BH and FDA wrote the paper. All authors read, gave comments, and approved the final version of the manuscript. The authors reported no potential conflicts of interest.

Reference List

- (1) Kuppers R. The biology of Hodgkin's lymphoma. *Nat Rev Cancer* 2009;9 (1):15-27.
- (2) Ferme C, Mounier N, Casasnovas O et al. Long-term results and competing risk analysis of the H89 trial in patients with advanced-stage Hodgkin lymphoma: a study by the Groupe d'Etude des Lymphomes de l'Adulte (GELA). *Blood* 2006;107 (12):4636-4642.
- (3) Dave SS, Wright G, Tan B et al. Prediction of survival in follicular lymphoma based on molecular features of tumor-infiltrating immune cells. *N Engl J Med* 2004;351 (21):2159-2169.
- (4) Sanchez-Aguilera A, Montalban C, de la CP et al. Tumor microenvironment and mitotic checkpoint are key factors in the outcome of classic Hodgkin lymphoma. *Blood* 2006;108 (2):662-668.
- (5) Steidl C, Lee T, Shah SP et al. Tumor-associated macrophages and survival in classic Hodgkin's lymphoma. *N Engl J Med* 2010;362 (10):875-885.
- (6) Chen G, Gharib TG, Huang CC et al. Discordant protein and mRNA expression in lung adenocarcinomas. *Mol Cell Proteomics* 2002;1 (4):304-313.
- (7) Ma Y, Visser L, Roelofsen H et al. Proteomics analysis of Hodgkin lymphoma: identification of new players involved in the cross-talk between HRS cells and infiltrating lymphocytes. *Blood* 2008;111 (4):2339-2346.
- (8) Wallentine JC, Kim KK, Seiler CE, III et al. Comprehensive identification of proteins in Hodgkin lymphoma-derived Reed-Sternberg cells by LC-MS/MS. *Lab Invest* 2007;87 (11):1113-1124.

- (9) Rabinovich GA, Toscano MA. Turning 'sweet' on immunity: galectin-glycan interactions in immune tolerance and inflammation. *Nat Rev Immunol* 2009;9 (5):338-352.
- (10) Rubinstein N, Alvarez M, Zwirner NW et al. Targeted inhibition of galectin-1 gene expression in tumor cells results in heightened T cell-mediated rejection; A potential mechanism of tumor-immune privilege. *Cancer Cell* 2004;5 (3):241-251.
- (11) Gandhi MK, Moll G, Smith C et al. Galectin-1 mediated suppression of Epstein-Barr virus specific T-cell immunity in classic Hodgkin lymphoma. *Blood* 2007;110 (4):1326-1329.
- (12) Juszczynski P, Ouyang J, Monti S et al. The AP1-dependent secretion of galectin-1 by Reed Sternberg cells fosters immune privilege in classical Hodgkin lymphoma. *Proc Natl Acad Sci U S A* 2007;104 (32):13134-13139.
- (13) Rodig SJ, Ouyang J, Juszczynski P et al. AP1-dependent galectin-1 expression delineates classical hodgkin and anaplastic large cell lymphomas from other lymphoid malignancies with shared molecular features. *Clin Cancer Res* 2008;14 (11):3338-3344.
- (14) Stein H, Delsol G, Pileri S. Classical Hodgkin lymphoma pathology and genetics of tumours of haemopoietic and lymphoid tissues. Lyon, France: IARC Press; 2001;244-253.
- (15) Cheson BD, Horning SJ, Coiffier B et al. Report of an international workshop to standardize response criteria for non-Hodgkin's lymphomas. NCI Sponsored International Working Group. *J Clin Oncol* 1999;17 (4):1244.
- (16) Honore B, Ostergaard M, Vorum H. Functional genomics studied by proteomics. *Bioessays* 2004;26 (8):901-915.

- (17) Vorum H, Ostergaard M, Hensechke P, Enghild JJ, Riazati M, Rice GE. Proteomic analysis of hyperoxia-induced responses in the human choriocarcinoma cell line JEG-3. *Proteomics* 2004;4 (3):861-867.
- (18) Mortz E, Krogh TN, Vorum H, Gorg A. Improved silver staining protocols for high sensitivity protein identification using matrix-assisted laser desorption/ionization-time of flight analysis. *Proteomics* 2001;1 (11):1359-1363.
- (19) Honore B, Buus S, Claesson MH. Identification of differentially expressed proteins in spontaneous thymic lymphomas from knockout mice with deletion of p53. *Proteome Sci* 2008;6:18.
- (20) Perkins DN, Pappin DJ, Creasy DM, Cottrell JS. Probability-based protein identification by searching sequence databases using mass spectrometry data. *Electrophoresis* 1999;20 (18):3551-3567.
- (21) Colell A, Green DR, Ricci JE. Novel roles for GAPDH in cell death and carcinogenesis. *Cell Death Differ* 2009;16 (12):1573-1581.
- (22) Dumontet C, Jordan MA. Microtubule-binding agents: a dynamic field of cancer therapeutics. *Nat Rev Drug Discov* 2010;9 (10):790-803.
- (23) Ferguson RE, Carroll HP, Harris A, Maher ER, Selby PJ, Banks RE. Housekeeping proteins: a preliminary study illustrating some limitations as useful references in protein expression studies. *Proteomics* 2005;5 (2):566-571.

- (24) Gulley ML, Glaser SL, Craig FE et al. Guidelines for interpreting EBER in situ hybridization and LMP1 immunohistochemical tests for detecting Epstein-Barr virus in Hodgkin lymphoma. *Am J Clin Pathol* 2002;117 (2):259-267.
- (25) Tzankov A, Went P, Zimpfer A, Dirnhofer S. Tissue microarray technology: principles, pitfalls and perspectives--lessons learned from hematological malignancies. *Exp Gerontol* 2005;40 (8-9):737-744.
- (26) Gundersen HJ, Bagger P, Bendtsen TF et al. The new stereological tools: disector, fractionator, nucleator and point sampled intercepts and their use in pathological research and diagnosis. *APMIS* 1988;96 (10):857-881.
- (27) Barrionuevo P, Beigier-Bompadre M, Ilarregui JM et al. A novel function for galectin-1 at the crossroad of innate and adaptive immunity: galectin-1 regulates monocyte/macrophage physiology through a nonapoptotic ERK-dependent pathway. *J Immunol* 2007;178 (1):436-445.
- (28) Correa SG, Sotomayor CE, Aoki MP, Maldonado CA, Rabinovich GA. Opposite effects of galectin-1 on alternative metabolic pathways of L-arginine in resident, inflammatory, and activated macrophages. *Glycobiology* 2003;13 (2):119-128.
- (29) Ilarregui JM, Croci DO, Bianco GA et al. Tolerogenic signals delivered by dendritic cells to T cells through a galectin-1-driven immunoregulatory circuit involving interleukin 27 and interleukin 10. *Nat Immunol* 2009;10 (9):981-991.
- (30) Garin MI, Chu CC, Golshayan D, Cernuda-Morollon E, Wait R, Lechler RI. Galectin-1: a key effector of regulation mediated by CD4+CD25+ T cells. *Blood* 2007;109 (5):2058-2065.

- (31) Duncan MW, Hunsucker SW. Proteomics as a tool for clinically relevant biomarker discovery and validation. *Exp Biol Med (Maywood)* 2005;230 (11):808-817.
- (32) Antonucci F, Chilosi M, Santacatterina M, Herbert B, Righetti PG. Proteomics and immunomapping of reactive lymph-node and lymphoma. *Electrophoresis* 2002;23 (2):356-362.
- (33) Antonucci F, Chilosi M, Parolini C, Hamdan M, Astner H, Righetti PG. Two-dimensional molecular profiling of mantle cell lymphoma. *Electrophoresis* 2003;24 (14):2376-2385.
- (34) Smith C, Beagley L, Khanna R. Acquisition of polyfunctionality by Epstein-Barr virus-specific CD8+ T cells correlates with increased resistance to galectin-1-mediated suppression. *J Virol* 2009;83 (12):6192-6198.
- (35) Toscano MA, Bianco GA, Ilarregui JM et al. Differential glycosylation of TH1, TH2 and TH-17 effector cells selectively regulates susceptibility to cell death. *Nat Immunol* 2007;8 (8):825-834.
- (36) Kamper P, Bendix K, Hamilton-Dutoit S, Honore B, Nyengaard JR, d'Amore F. Tumor-infiltrating macrophages correlate with adverse prognosis and Epstein-Barr virus status in classical Hodgkin's lymphoma. *Haematologica* 2011;96 (2):269-276.
- (37) Steidl C, Farinha P, Gascoyne RD. Macrophages predict treatment outcome in Hodgkin's lymphoma. *Haematologica* 2011;96 (2):186-189.
- (38) Shau H, Gupta RK, Golub SH. Identification of a natural killer enhancing factor (NKEF) from human erythroid cells. *Cell Immunol* 1993;147 (1):1-11.

- (39) Neumann CA, Krause DS, Carman CV et al. Essential role for the peroxiredoxin Prdx1 in erythrocyte antioxidant defence and tumour suppression. *Nature* 2003;424 (6948):561-565.

- (40) Ghosh P, Garcia-Marcos M, Bornheimer SJ, Farquhar MG. Activation of Galphai3 triggers cell migration via regulation of GIV. *J Cell Biol* 2008;182 (2):381-393.

- (41) van Haastert PJ, Devreotes PN. Chemotaxis: signalling the way forward. *Nat Rev Mol Cell Biol* 2004;5 (8):626-634.

- (42) Aldinucci D, Gloghini A, Pinto A, De FR, Carbone A. The classical Hodgkin's lymphoma microenvironment and its role in promoting tumour growth and immune escape. *J Pathol* 2010;221 (3):248-263.

- (43) Gribben JG. Implications of the tumor microenvironment on survival and disease response in follicular lymphoma. *Curr Opin Oncol* 2010;22 (5):424-430.

Table 1. Clinical characteristics of patients selected for proteome comparison

No.	Age, years	Histology	Ann Arbor Stage	B symptoms	Treatment	Outcome
1	21	MC	III	absent	ABVD	FR
2	24	NS	II	present	ABVD/COPP+RT	FR
3	24	NS	IV	present	ABVD/COPP	FR
4	26	NS	II	present	ABVD/COPP+RT	FR
5	35	NS	III	absent	ABVD+RT	FR
6	20	NS	III	present	ABVD/COPP+RT	FR
7	25	NS	III	present	ABVD/COPP+RT	FR
8	51	cHL-NOS	I	present	ABVD/COPP+RT	UR
9	41	NS	IV	present	ABVD/COPP+RT	UR
10	14	NS	III	present	ABVD/COPP	UR
11	21	NS	II	present	ABVD/COPP	UR
12	27	NS	II	present	ABVD/COPP	UR
13	33	NS	IV	present	ABVD	UR
14	23	NS	III	present	ABVD/COPP+RT	UR

Abbreviations: FR, Favorable response; UR, Unfavorable response; MC, mixed cellularity; NS, Nodular sclerosis; cHL –NOS, classical Hodgkin lymphoma – not otherwise specified; ABVD/COPP, adriamycin, bleomycin, vinblastine, dacarbazine/cyclophosphamide, vincristin, procarbazine, prednisone; RT, radiotherapy

Table 2. List of identified proteins.

Spot no.	Identified peptides	Protein name	SwissProt accession	Size (kDa)	Mascot score	Biological processes**
pH 3-10						
1507	DREVGIPPEQSLETAK EFNKYDTDGSK	Actin-related protein 3	ARP3_HUMAN	47.4	77	Cellular component movement, regulation of actin filament polymerization, activation of dendrite morphogenesis, regulation of myosin II filament assembly or disassembly, response to antibiotic
2002	DGGVQACFSRSR	Guanine nucleotide-binding protein G(k) subunit alpha	GNAI3_HUMAN	40.5	24***	G protein coupled receptor protein signaling pathway, negative regulation of adenylate cyclase activity, negative regulation of synaptic transmission, signal transduction, vesicle function
2102	VRGEVAPDAK FNAHGDAANTIVCNSK	Galectin-1	LEG1_HUMAN	14.7	154	Activation of I-kB kinase/NF-kB cascade, apoptotic programmed cell death, cellular response to glucose stimulus, multicellular organismal response to stress, myoblast cell differentiation, negative regulation of cell-substrate adhesion
3102	QEYDESGPSIVHR	Actin****	ACTB_HUMAN	42	86	Blood coagulation, platelets activation, platelets degranulation
3107	TCVADESAENCDK	Serum albumin	ALBU_HUMAN	69.4	23***	Transport, negative regulation of programmed cell death and apoptosis, maintenance of mitochondrial location, cellular response to starvation
3107	HHEASSRADSSR	Filaggrin	FILA_HUMAN	435	32	Keratinocyte differentiation, multicellular organismal development
4103	GSPAINVAHVFR	Transthyretin	TTHY_HUMAN	16	96	Transport
4302*	AGVETTTPSK	Ig lambda chain C regions	LAC_HUMAN	11.3	65	Involved in immune response
4302*	QEYDESGPSIVHR	Actin****	ACTB_HUMAN	42	87	Blood coagulation, platelets activation, platelets degranulation
4502	DSYVGDEAQS K DSYVGDEAQS K VAPEEHPVLLTEAPLNPK LCYVALDFEQEMATAASSSLEK SYELPDGQVITIGNER DLYANTVLSGGTMYPGIADR QEYDESGPSIVHR	Actin****	ACTG_HUMAN	42	601	Adherens junctions organization, axon guidance, cell junction assembly, cell-cell junction organization, cellular component movement, response to calcium ion
5402	LIAPVAEEEEATVPNNK SLADELALVDVLEDK VIGSGCNLDSAR LKDDEVAQLKK	L-lactate dehydrogenase B chain	LDHB_HUMAN	37	298	Cellular carbohydrate metabolic process, glycolysis, lactate metabolic process NAD metabolic process, oxidation-reduction process, pyruvate metabolic process
5403	IEDGNNFGVAVQEK QPHVGDYR	Proteasome activator complex subunit 1	PSME1_HUMAN	28.7	136	Regulation of ubiquitin-protein ligase activity involved in mitotic cell cycle, proteasomal ubiquitin-dependent protein catabolism
5604*	DSYVGDEAQS K DSYVGDEAQS K	Actin****	ACTA_HUMAN	42	85	Muscle contraction, regulation of blood pressure, response to virus, vascular smooth muscle contraction
5604*	ALLQAILQTEDMLK ETQSQLETER	Desmoplakin	DESP_HUMAN	331.8	37	Adherens junction organization, cell-cell adhesion, development of epidermis, keratinocyte differentiation, peptide cross-linking, wound healing

5708	AAPEASGTPSSDAVSR	Coronin-1A	COR1A_HUMAN	51.0	52	Actin modulating activity, calcium ion transport, cell-substrate adhesion, cell movement, involved in immune response (t cell response, t cell homeostasis, leukocyte chemotaxis, phagocytosis), regulation of cell shape
6002	VHLTPEEK VNVDEVGGALGR	Hemoglobin subunit beta	HBB_HUMAN	16.0	105	Nitric oxide transport, oxygen transport, regulation of nitric oxide biosynthesis, regulation of blood pressure, regulation of blood vessel size.
8103	AGAHLQGGAK	Glyceraldehyde-3-phosphate dehydrogenase	G3P_HUMAN	36	39	Glucose metabolism, glycolysis, oxidation and reduction processes
8206	ATAVMPDGQFK	Peroxiredoxin-1	PRDX1_HUMAN	22.1	30	Cell. Proliferation, cell redox homeostasis, erythrocyte homeostasis, hydrogen peroxide catabolic process, NK cell mediated cytotoxicity, oxidation and reduction processes, regulation of NF-kappaB import into nucleus, regulation of stress-activated MAPK cascade, removal of superoxide radicals, skeletal system development
8208*	IGHPAPNFK ATAVMPDGQFK QITVNDLPVGR	Peroxiredoxin-1	PRDX1_HUMAN	22.1	25***	Cell. Proliferation, cell redox homeostasis, erythrocyte homeostasis, hydrogen peroxide catabolic process, NK cell mediated cytotoxicity, oxidation and reduction processes, regulation of NF-kB import into nucleus, regulation of stress-activated MAPK cascade, removal of superoxide radicals, skeletal system development
8208*	AGVETTPSK	Ig lambda chain C regions	LAC_HUMAN	11.3	32***	Involved in immune response
9002	DLYANTVLSGGTMYPGIADR	Actin****	ACTB_HUMAN	42	99	Blood coagulation, platelets activation, platelets degranulation
9201	LVIINGNPITIFQER AGAHLQGGAK IISNASCTTNCLAPLAK	Glyceraldehyde-3-phosphate dehydrogenase	G3P_HUMAN	36	186	Glucose metabolism, glycolysis, oxidation and reduction processes
7505	TCVADESAENCDK ETYGEMADCCAK AAFTECCQAADK	pH 4-7 Serum albumin	ALBU_HUMAN	69.4	182	Transport, negative regulation of programmed cell death and apoptosis, maintenance of mitochondrial location, cellular response to starvation
3105	GCITIIGGGDTATCCAK	Phosphoglycerate kinase 1	PGK1_HUMAN	45	55	Carbohydrate metabolic process, gluconeogenesis, glucose metabolic process, glycolysis, phosphorylation
3505	VAPEEHPVLLTEAPLNPK	Actin****	ACTB_HUMAN	42	60	Blood coagulation, platelets activation, platelets degranulation
3704	SYELPDGQVITIGNER	Actin****	ACTA_HUMAN	42	56	Muscle contraction, regulation of blood pressure, response to virus, vascular smooth muscle contraction
7301	VAPEEHPVLLTEAPLNPK	Actin****	ACTB_HUMAN	42	73	Blood coagulation, platelets activation, platelets degranulation

* LC-MS/MS and subsequent search in the Swiss-Prot Database resulted in more than one possible protein identification

** Biological processes are taken from the Gene Ontology (GO) annotation system

*** Identifications are significant when searches are performed in the human part of the SwissProt database

**** Several actin isoforms can be identified from the peptides

Table 3. Correlation of demographic and clinico-pathological parameters with Gal-1 expression in the HRS cells and in the tumor microenvironment.

Characteristic	Total no.	%	HRS Gal-1		P*	Non-HRS Gal-1	
			Gal-1 neg	Gal-1 pos		cell profile Gal-1 count/mm ²	Median
	143						
Age, years (n=143)							
<45	91	64	46	45	0.11*	1361	0.27
≥45	52	36	19	33		1496	
Sex (n=143)							
Male	92	64	43	49	0.68*	1387	0.30
Female	51	36	22	29		1361	
Ann Arbor Stage (n=143)							
I-II	57	40	23	34	0.32*	1511	0.62
III-IV	86	60	42	44		1358	
B symptoms (n=143)							
Yes	117	82	46	71	0.002*	1482	0.03
No	26	18	19	7		1138	
Bulky disease (>10cm) (n=135)¹							
Yes	49	36	23	26	0.76*	1228	0.20
No	86	64	38	48		1377	
Histologic type (n=143)							
NSI	78	55	37	41	0.03**	1523	0.49
NSII	42	29	13	29		1302	
MC	22	15	15	7		1387	
cHL, NOS	1	1	0	1		1523	
IPS (n=125)¹							
≤ 2	68	54	36	32	0.11*	1369	0.51
> 2	57	46	22	35		1361	
EBV status (n=143)							
Positive	48	34	28	20	0.03*	1345	0.54
Negative	95	66	36	32		1384	

¹ Parameter not available in all 143 patients; *Chi2-test; ** Wilcoxon rank-sum test or Kruskal-Wallis equality-of-populations rank test where appropriate ; Abbreviations: HRS, Hodgkin/Reed-Sternberg cells; NSI and NSII, nodular sclerosis type I and II; MC, mixed cellularity; cHL, NOS, classical Hodgkin lymphoma, not otherwise specified; IPS, international prognostic score; EBV, Epstein-Barr virus

Table 4 Correlation of clinico-pathological parameters and Gal-1 expression in non-neoplastic cells with survival

Characteristic	Overall Survival				Event-free Survival			
	5-Year OS (%)	HR	95 % CI	p	5-Year EFS (%)	HR	95 % CI	p
Age, yrs								
<45	92	1	ref	<0.001	64	1	ref	0.005
≥45	57	5.36	2.86-10.06		48	1.91	1-21-3.01	
Sex								
Male	78	1	ref	0.16	55	1	ref	0.09
Female	80	1.55	0.84-2.90		63	1.52	0.94-2.46	
Ann Arbor Stage								
I-II	80	1	ref	0.87	63	1	ref	0.33
III-IV	77	0.95	0.53-1.72		55	1.26	0.79-2.01	
B symptoms								
No	79	1	ref	0.45	60	1	ref	0.84
Yes	79	1.37	0.61-3.07		52	0.94	0.54-1.66	
Bulky disease (>10cm)								
Yes	71	1	ref	0.15	60	1	ref	0.27
No	82	1.57	0.85-2.92		54	1.31	0.81-2.11	
Histologic type								
NSI	84	1	ref	0.21	64	1	ref	0.13
NSII	70	1.43	0.72-2.82		56	1.19	0.69-2.04	
MC	77	1.11	0.45-2.72		49	1.47	0.77-2.79	
cHL, NOS	33	4.50	1.05-19.35		0	3.77	1.16-12.3	
EBV status								
neg.	78	1	ref	0.77	57	1	ref	0.86
pos.	79	1.09	0.59-2.03		60	0.96	0.59-1.55	
Gal-1 (all)								
Low	81	1	ref	0.06	62	1	ref	0.02
High	70	1.87	0.97-3.60		45	1.85	1.11-3.09	
Gal-1 (< 61 yrs)								
Low	90	1	ref		69	1	ref	
High	78	3.25	1.38-7.67	0.007	49	2.34	1.26-4.36	0.007

Abbreviations: NSI and NSII, nodular sclerosis type I and II; MC, mixed cellularity; cHL, NOS, classical Hodgkin lymphoma not otherwise specified; NLPHL, nodular lymphocyte predominant Hodgkin lymphoma; IPS, international prognostic score; EBV, Epstein-Barr virus

Figure Legends:

Figure 1

Flowchart describing the two-step study strategy (training-set followed by validation-set analysis).

2D-PAGE= two-dimensional polyacrylamide gel electrophoresis; LC-MS/MS=liquid chromatography-mass spectrometry/mass spectrometry; WB=Western blot; IHC=immunohistochemistry; HRS=Hodgkin/Reed-Sternberg; Gal-1=galectin-1;

Figure 2

(A-B) Representative gels (pH 3-10 IPG and pH 4-7 IPG) from two-dimensional polyacrylamide gel electrophoresis (2D-PAGE). Four digit numbers are the specific spot numbers of the proteins listed in Table 2. **(C)** Histograms of all identified proteins displaying the spot intensities. Each patient is represented by one column and columns are stacked according to treatment response (favourable versus unfavourable outcome).

Figure 3

(A) Western blots of differentially expressed proteins and **(B)** dotplots demonstrating the band intensities according to treatment outcome.

Figure 4

Representative immunohistochemical stainings of the differentially expressed proteins Gal-1, PSME-1 and PRDX-1 (x 400). **(A)** Gal-1 staining of a multinuclear HRS cell (thick arrow). **(B)** PSME-1 staining of HRS cells (thick arrow) and tumor-infiltrating cells. **(C)** PRDX1 staining showing a positive HRS cell (thick arrow) among PRDX-1-positive macrophages (thin arrow).

Figure 5

Overall survival (OS) and event-free survival (EFS) according to Gal-1 expression. **(A-B)** Analysis including all patients (n=143), **(C-D)** Analysis restricted to younger patients (< 61 years, n=112).

HR=hazard ratio.

Fig.1

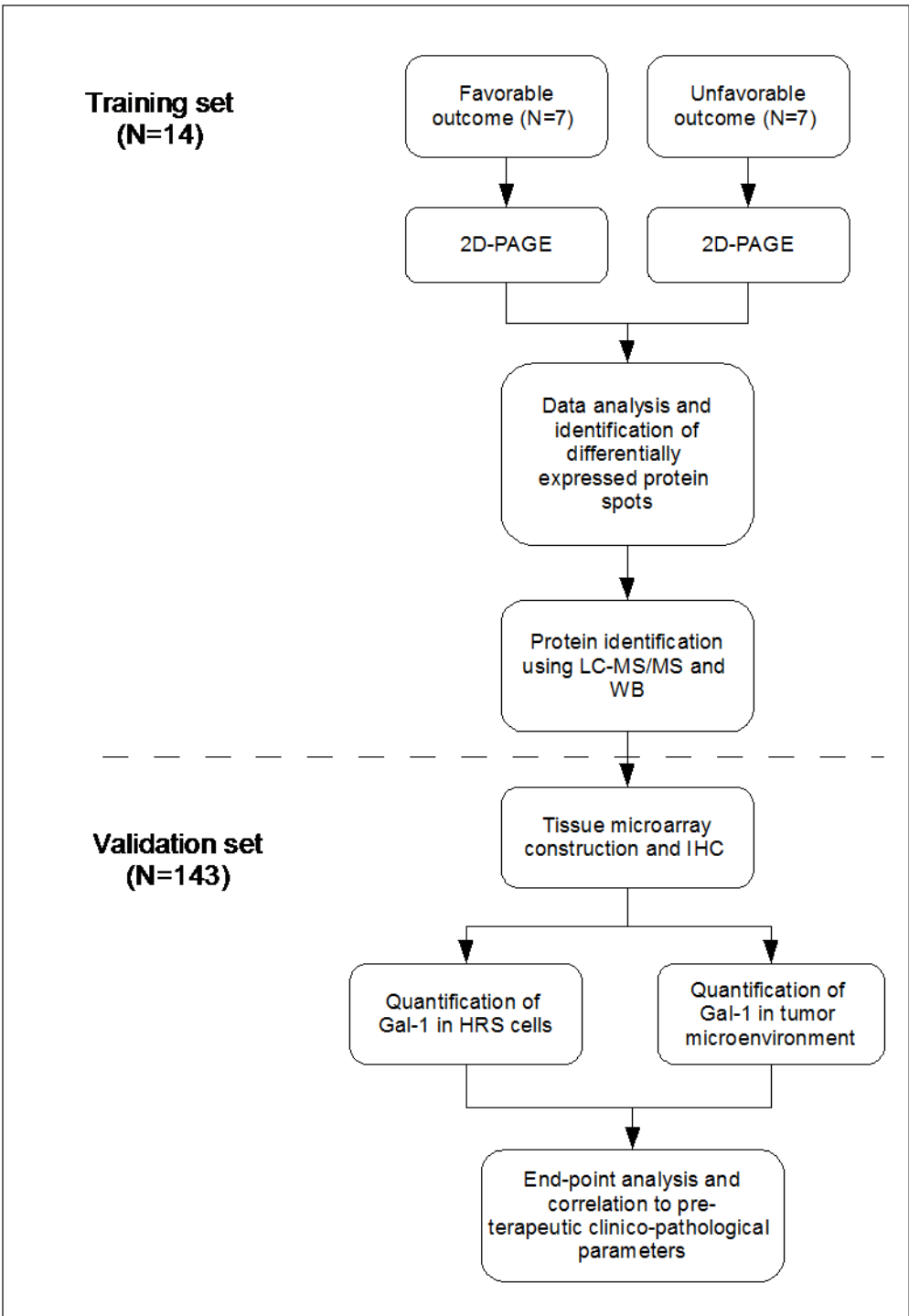


Fig.2

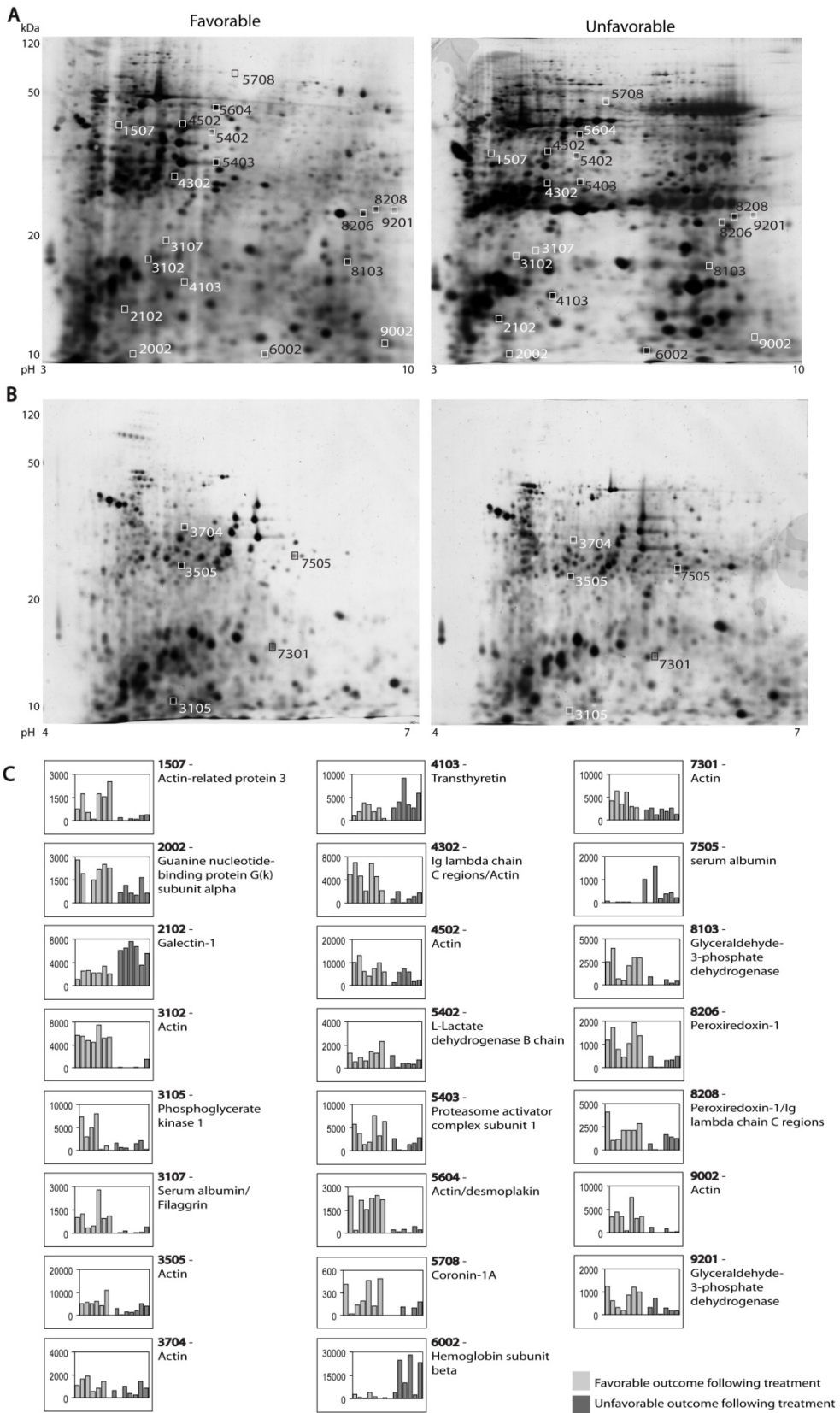


Fig.3

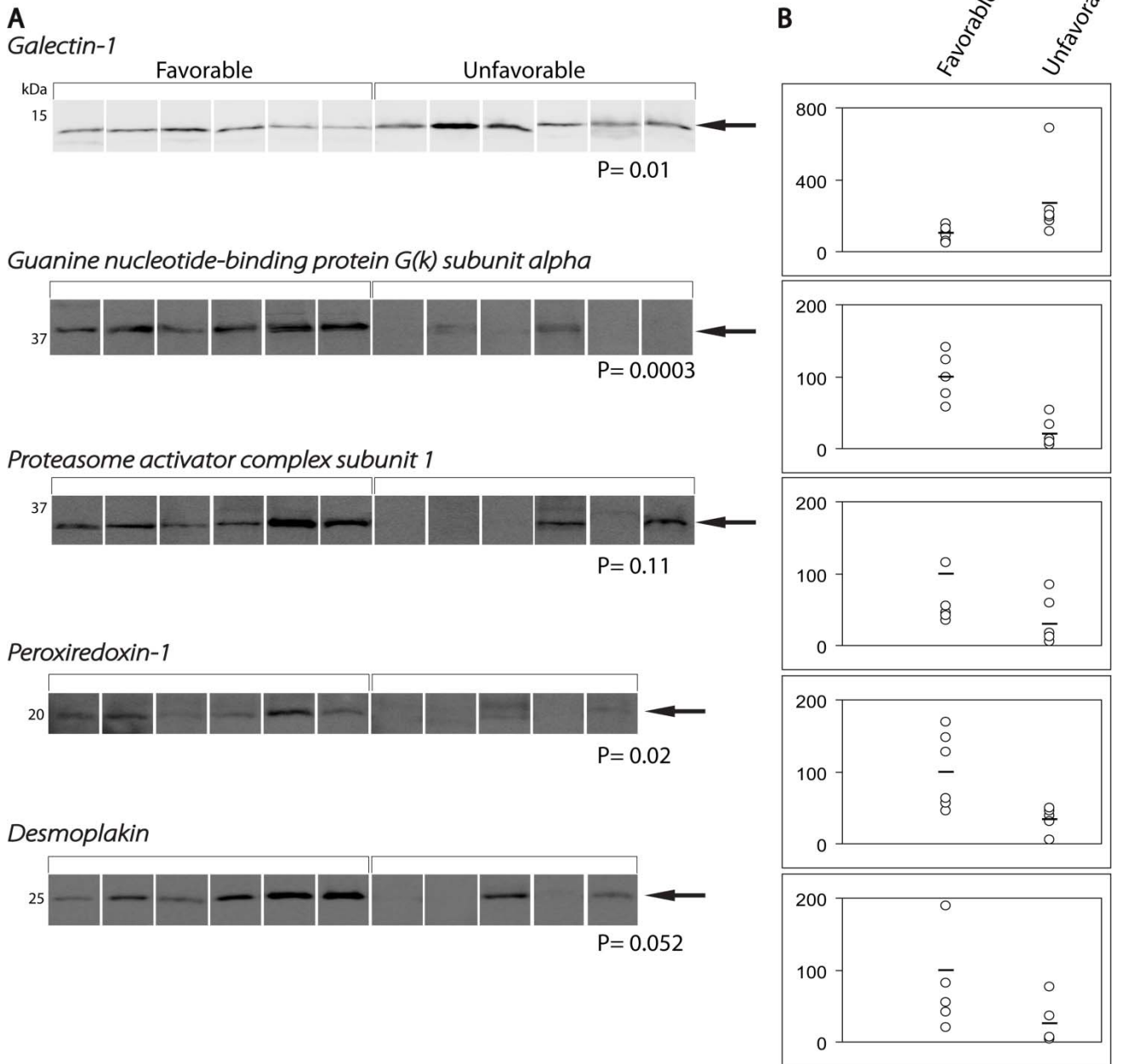
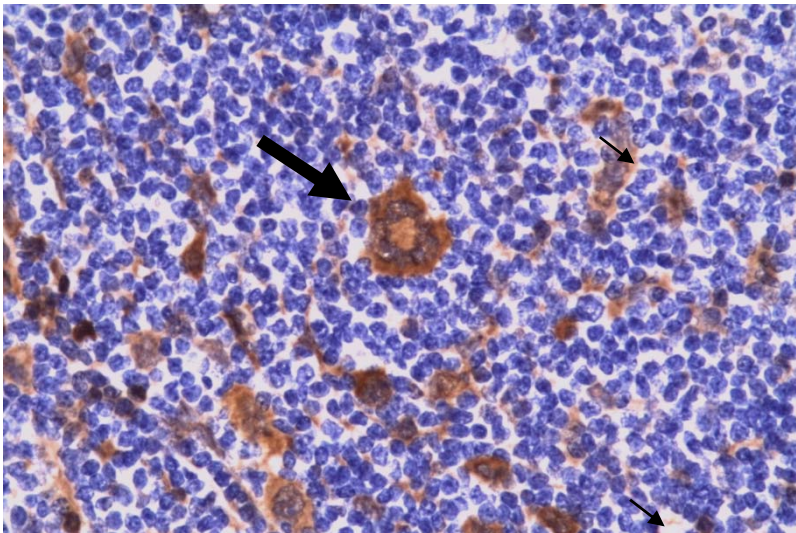
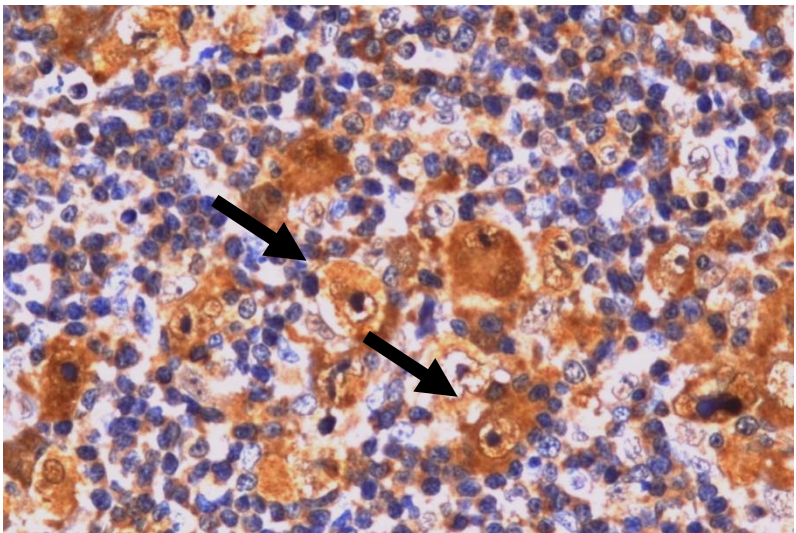


Fig. 4

A



B



C

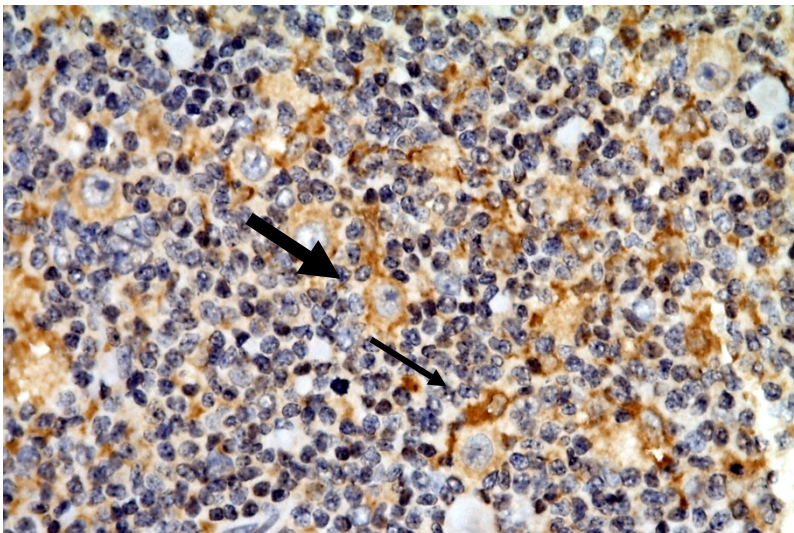
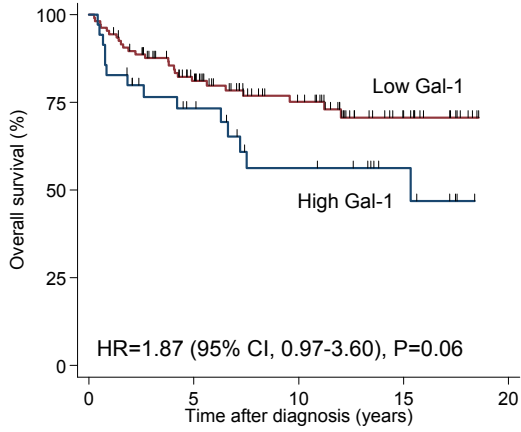


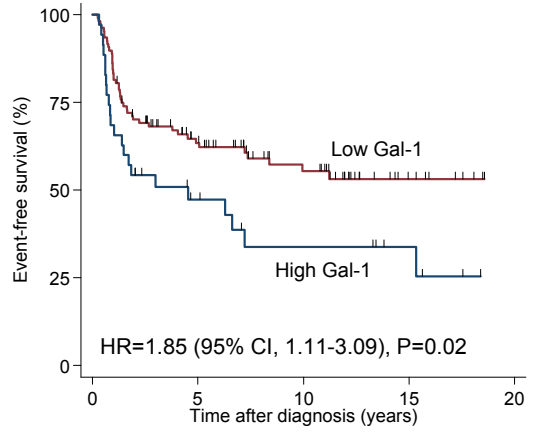
Fig.5

A OS according to Gal-1 expression (all patients, n=143)



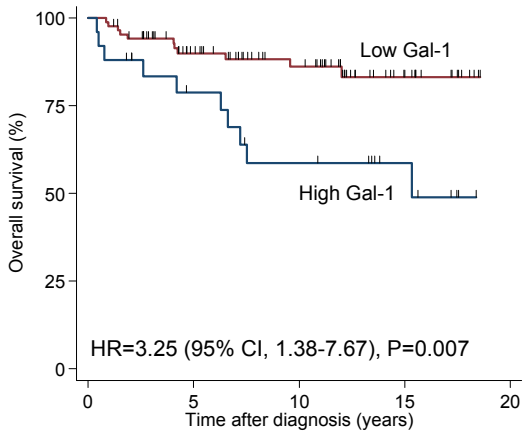
Number at risk		0	5	10	15	20
Low Gal-1	108	69	42	15	0	
High Gal-1	35	20	12	6	0	

B EFS according to Gal-1 expression (all patients, n=143)



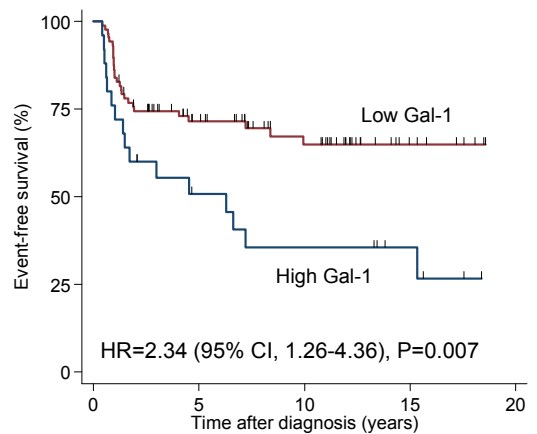
Number at risk		0	5	10	15	20
Low Gal-1	108	52	30	8	0	
High Gal-1	35	12	7	4	0	

C OS according to Gal-1 expression (patients ≤ 61 yrs, n=112)



Number at risk		0	5	10	15	20
Low Gal-1	87	59	40	14	0	
High Gal-1	25	16	11	6	0	

D EFS according to Gal-1 expression (patients ≤ 61 yrs, n=112)



Number at risk		0	5	10	15	20
Low Gal-1	87	45	28	7	0	
High Gal-1	25	10	7	4	0	